BBA - Biomembranes 1861 (2019) 130–141

Contents lists available at ScienceDirect

BBA - Biomembranes

journal homepage: www.elsevier.com/locate/bbamem

The use of styrene-maleic acid copolymer (SMA) for studies on T cell membrane rafts

Pavla Angelisová[a], Ondřej Ballek[a], Jan Sýkora[b], Oldřich Benada[c], Tomáš Čajka[d], Jana Pokorná[a], Dominik Pinkas[a], Václav Hořejší[a,*]

[a] Institute of Molecular Genetics of the Czech Academy of Sciences, Vídeňská 1083, 142 20 Praha 4, Czech Republic
[b] J. Heyrovský Institute of Physical Chemistry of the Czech Academy of Sciences, Dolejškova 2155/3, 182 23 Prague 8, Czech Republic
[c] Institute of Microbiology of the Czech Academy of Sciences, Vídeňská 1083, 142 20 Praha, 4, Czech Republic
[d] Institute of Physiology of the Czech Academy of Sciences, Vídeňská 1083, 142 20 Praha 4, Czech Republic

ARTICLE INFO

Keywords:
Membrane rafts
SMA
GPI-anchored proteins
T lymphocytes
Src family kinases
Membrane proteins

ABSTRACT

An emerging alternative to the use of detergents in biochemical studies on membrane proteins is apparently the use styrene-maleic acid (SMA) amphipathic copolymers. These cut the membrane into nanodiscs (SMA-lipid particles, SMALPs), which contain membrane proteins possibly surrounded by their native lipid environment. We examined this approach for studies on several types of T cell membrane proteins, previously defined as raft or non-raft associated, to see whether the properties of the raft derived SMALPs differ from non-raft SMALPs. Our results indicate that two types of raft proteins, GPI-anchored proteins and two Src family kinases, are markedly present in membrane fragments much larger (> 250 nm) than those containing non-raft proteins (< 20 nm). Lipid probes sensitive to membrane fluidity (membrane order) indicate that the lipid environment in the large SMALPs is less fluid (more ordered) than in the small ones which may indicate the presence of a more ordered lipid L_o phase which is characteristic of membrane rafts. Also the lipid composition of the small vs. large SMALPs is markedly different – the large ones are enriched in cholesterol and lipids containing saturated fatty acids. In addition, we confirm that T cell membrane proteins present in SMALPs can be readily immunoisolated. Our results support the use of SMA as a potentially better (less artifact prone) alternative to detergents for studies on membrane proteins and their complexes, including membrane rafts.

1. Introduction

It has been firmly established that cell membranes exhibit lateral heterogeneity – lipids and proteins apparently form “microdomains” or “nanodomains” of various size and stability, transmembrane domains of proteins associate with specific lipids forming lipid shells, peripheral membrane proteins and submembrane cytoskeletal elements preferentially associate with certain membrane lipid species. Particular attention has been paid to a type of microdomains called membrane rafts selectively concentrating a specific set of functionally relevant proteins (mostly lipidated) and (glyco)lipids (recently reviewed in [1]). Biochemical studies on membrane rafts have been mostly based on their apparent selective resistance to solubilization by some detergents, e.g. Triton X100, Brij-series, NP-40 or CHAPS [2,3]. Detergent-resistant membrane fragments (DRMs) which are produced by membrane disintegration by these detergents have been for some time considered to be equivalent to membrane rafts which exist in membranes before solubilization. The relative resistance to detergent solubilization has been explained by the presence of a relatively compact ordered liquid phase which is formed by prevalent lipids that contain saturated fatty acid residues and cholesterol [4]. Indeed, treatment of membranes with cholesterol-depleting agents [5], cholesterol-modifying enzymes or biosynthetic replacement of saturated fatty acid residues in their sphingolipids by unsaturated ones [6] were found to destabilize the rafts resulting in the loss of detergent resistance. More recently, it has become obvious that the use of such detergents may produce significant artefacts – the composition and properties of the DRMs were clearly dependent on the chemical nature and concentration of the detergent, temperature, and duration of solubilization [7–9]. Thus, the present consensus is that DRMs generally should no longer be considered as biochemical equivalents of native rafts, the results based on DRMs should be interpreted with caution [9] and complemented with other more physiological approaches such as the use of plasma membrane vesicles [10].

* Corresponding author.
E-mail address: vaclav.horejsi@img.cas.cz (V. Hořejší).

https://doi.org/10.1016/j.bbamem.2018.08.006
Received 18 January 2018; Received in revised form 9 August 2018; Accepted 13 August 2018
Available online 14 August 2018
0005-2736/ © 2018 Elsevier B.V. All rights reserved.

Because of the well substantiated criticism as to the use of specific detergents for isolation and biochemical studies of DRMs, alternative methods for the disintegration of cell membranes that would minimally perturb the native arrangement of the membrane rafts are desirable. A promising alternative to detergents which is based on the use of styrene-maleic acid (SMA) amphipatic copolymers [11,12] has been recently implemented in membrane research. SMA molecules spontaneously integrate within membrane cutting them into "nanodiscs" while the polymer forms an annulus that surrounds and stabilizes, in a presumably native state, a small area of lipid bilayer (approx. 12 nm diameter). The phenyl moieties of the copolymer are apparently intercalated between the lipid molecules and the carboxy groups likely interact with the aqueous environment and to some extent may also interact with lipid polar headgroups [13,14]. This model is supported by small angle neutron scattering data, electron microscopy, attenuated total reflection Fourier transform infrared spectroscopy, differential scanning calorimetry and nuclear magnetic resonance spectroscopy [15]. The nanodiscs are stable entities, which are also known as SMA-lipid particles (SMALPs) that do not require the presence of a free soluble copolymer in solution. The proteins that are associated with native nanodiscs thus essentially behave like soluble proteins. Several membrane proteins and their complexes have been successfully purified from SMA-solubilized membranes [13,14,16–20].

Membrane rafts of leukocytes are of great interest because they contain several important signaling molecules that are involved in immunoreceptor signaling [21,22].

In the present study, we explored the use of SMA for solubilization of T lymphocyte membranes. We wondered whether this type of membrane disintegration would also indicate a different behavior of typical raft and non-raft T lymphocyte proteins, as previously described in studies that employed certain detergents.

2. Materials and methods

2.1. Reagents

The following reagents were obtained from the indicated commercial sources: Brij-98 (Sigma-Aldrich), laurylmaltoside (Calbiochem), SMA sodium salt (Lipodisq™ Pre-Hydrolysed P(SMA) (3:1 Ratio); m.w. 9,5 kDa; Malvern Pharmaceuticals), concanavalin A (Con A)-horse radish peroxidase (HRP) and cholera toxin-HRP conjugates (Sigma-Aldrich), benzonase (Novagen), 6-dodecanoyl-*N*,*N*-dimethyl-2-naphthylamine (Laurdan) (Thermo Fischer Scientific), 1,6-diphenyl-1,3,5-hexatriene (DPH) (Sigma-Aldrich).

2.2. Cells and antibodies

Jurkat cells were obtained from ATCC. Six to eight weeks old C57BL/6J mice, housed in a specific pathogen-free animal facility of our institute, were used. Primary lymph node $CD4^+$ T-cells (~95% purity) were isolated from mice using a MACS $CD4^+$ T-cell isolation kit (AutoMACS, Miltenyi Biotec).

Rabbit polyclonal antibodies specific to human LAT and Lck and mouse Fyn were kindly provided by Dr. L. Samelson and Dr. A. Veillette, respectively, mAb βF1 to TCRβ were acquired from Dr. M. Brenner, and mAb IA10 to CD55 was provided by Dr. M. B. Whitlow. MAbs to human Fyn (FYN-01), human Lck (LCK-01), H-Ras (RAS-01), LAT (LAT-01), CD5 (MEM-32), CD45 (MEM-28), CD18 (MEM-48), CD48 (MEM-102), CD59 (MEM-43), CD147 (MEM-M6/1), as well as polyclonal rabbit antibodies to human PAG and CD59 were used for Western blotting immunostaining. These antibodies were prepared previously in our laboratory and are commercially available from EXBIO (Vestec, Czechia). Antibodies to the following molecules used for Western blotting immunostaining were obtained from the following commercial sources: CD3ζ (mAb 6B10.2, Santa Cruz), CD3ε (mAb Leu4, Ortho), mouse Lck (mAb 3A5, Millipore), mouse LAT (rabbit polyclonal, Cell Signaling), goat anti-mouse IgG-HRP, and goat anti-rabbit Ig-HRP (BioRad).

2.3. Jurkat cell membrane preparation [23]

Cells (1.5×10^8) were resuspended in 1 mL of ice-cold hypotonic buffer (10 mM HEPES pH 7.4, 42 mM KCl, 5 mM $MgCl_2$, protease inhibitor mixture), incubated on ice for 15 min. The suspension was then passed 8× through a 25- followed by 5× through a 30-gauge needle. The suspension was then centrifuged for 5 min at 580 ×*g* and 0 °C to remove nuclei. The post-nuclear supernatant was centrifuged for 10 min at 25,000 ×*g*, 2 °C to pellet the membranes. This preparation contains mostly plasma membrane fragments but also certain amounts of Golgi and ER membranes, as verified by Western blotting of relevant markers (data not shown).

2.4. Membrane and cell solubilization

Once the membranes were prepared (see Section 2.3), they were lysed in 1 mL of lysis buffer (20 mM Tris-HCl pH 8.2 containing 100 mM NaCl, 5 mM iodoacetamide, Protease Inhibitor Cocktail III (Calbiochem), 10 mM EDTA, 50 mM NaF, 10 mM $Na_4P_2O_7$ and 1% SMA (or in some experiments 3% SMA, 1% Brij-98 or 1% laurylmaltoside)), for 1 h at room temperature, if not stated otherwise. Alternatively, $1\text{-}5 \times 10^7$ Jurkat cells or mouse T cells were solubilized in the same way with 1% SMA; in this case 1 μL (25 U) of benzonase endonuclease solution and 10 μL of 1 M $MgCl_2$ was added to digest the viscous nuclear contents released by SMA. Such lysates were either used directly for density gradient ultracentrifugation (without removing insoluble components), or spun at 25,000 ×*g* for 3 min to remove nuclei and other insoluble materials, and used for gel filtration or immunoprecipitation.

2.5. Density gradient ultracentrifugation

This method that has been previously used in studies that have dealt with presumably raft-derived DRMs [2] is suitable for the separation of relatively large and low-density membrane fragments (presumably rich in lipids) from small and/or relatively dense macromolecules and molecular complexes. For this type of separation, placing the sample at the bottom of the gradient is optimal. This separation was conducted as previously described [24]. Briefly, the SMA membrane lysate (0.5 mL) or relevant fractions from gel filtration were added to 0.5 mL of 80% (wt/vol) sucrose in lysis buffer and placed at the bottom of a 5.2 mL centrifuge tube. The mixture was then carefully overlaid with 1.8 mL of 30%, 0.8 mL 20%, 0.8 mL 10% and 0.7 mL 5% sucrose in lysis buffer and finally with 0.1 mL of lysis buffer. Centrifugation was performed at 10 °C in a Beckman Optima MAX-E ultracentrifuge, using a MLS50 swing-out rotor (18 h, 50,000 rpm). Nine 0.58 mL fractions were collected gradually from the top of the gradient. Proteins were then separated by SDS-PAGE and analyzed by immunoblotting.

2.6. Sedimentation of SMALPs by ultracentrifugation

Large SMALPs present in the initial Sepharose 4B gel filtration fractions were subjected to ultracentrifugation at 60,000 rpm (approx. 135,000 ×*g*) for 1 h at 20 °C using a TLA 110 rotor in a Beckman Optima ultracentrifuge. The supernatant and sediment (adjusted to the original volume or concentrated 10×) were examined by SDS PAGE and Western blotting.

2.7. Gel filtration (size exclusion chromatography, SDS-PAGE and Western blotting)

This method was performed as previously described [24]. Briefly, 0.1 mL of the cell lysate (after nuclei removal by 3 min centrifugation at 25,000 ×*g*) or membrane lysate was applied on top of a 1 mL Sepharose

4B column (in lysis buffer without iodoacetamide, protease inhibitors and SMA) and washed with the same modified lysis buffer. The 0.1 mL fractions were collected (performed at room temperature) and analyzed by SDS-PAGE/immunoblotting. The initial fractions from this highly porous gel (fr. 4–6) contained large complexes or particles; a majority of mol. wt. standards IgM (900 kDa) and IgG (150 kDa) eluted in fractions 7 and 8–9, respectively, while large particles (erythrocytes) eluted in fraction 4 [25]. The lysates did not contain any glycerol that could possibly influence the results of gel filtration experiments.

SDS-PAGE (non-reduced boiled samples) and Western blotting were performed essentially as previously described [26]. The positions of the specific protein bands visualized by Western blotting in the respective figures correctly correspond to their approximate apparent "electrophoretic" m.w. (Lck - 55 kDa, Fyn - 55 kDa, LAT - 38 kDa, PAG - 70 kDa, H-Ras - 20 kDa, CD3ζ dimer - 32 kDa, CDε dimer - 38 kDa, TCRβ in the αβ heterodimer- 90 kDa, CD5 - 60 kDa, CD18 - 90 kDa, CD45 - 200 kDa, CD48 - 42 kDa, CD55 - 65 kDa, CD59 - 18 kDa, CD71 dimer - 180 kDa, CD147 - 75 kDa). The presented results of Western blotting are representative of at least three analogous experiments.

2.8. Sonication

Ice cooled samples were sonicated 3 × 20 s at amplitude 50, in Ultrosonic homogenizer 4710 (Cole Parmer Instruments).

2.9. Immunoprecipitation

A 60 μL suspension of Protein A/G PLUS-Sepharose (Santa Cruz Biotechnology) in PBS was incubated with 1–5 μg Ab per sample for 2 h at 4 °C, washed with the lysis buffer and the Ab-coated beads were rotated with 250 μL the Jurkat cell or membrane SMA lysate for 2 h at room temperature and washed on spin-columns (BioRad, 732-6204) with lysis buffer. Immunoisolated material was eluted with 2× concentrated non-reducing SDS-PAGE sample buffer and analyzed by Western blotting.

2.10. Dynamic light scattering

The dynamic light scattering (DLS) experiments were carried out at 20 °C on a Zetasizer Nano ZS (Malvern Instruments) using a He-Ne laser (532 nm) and an avalanche photodiode detector (APD). The scattering intensity was collected at an angle of 173°. Intensity-weighted size distributions were obtained using a regularized fitting implemented in Zetasizer Software 6.2 (Malvern). The DLS instrument was calibrated using 60 nm (NIST® SRM® 1964), 100 nm (NIST® SRM® 1963a) and 200 nm diameter polystyrene spheres dispersed in water (Sigma-Aldrich). The specific sizes of these standard microparticles were determined to be 63.8 ± 13.9 nm, 105.6 ± 17.8 nm, and 203.7 ± 44.2 nm, respectively. The polydispersity index for all the measurements did not exceed 0.05.

2.11. Steady-state fluorescence of Laurdan and DPH [27]

The gel filtration fractions from cell membranes that were disintegrated by SMA (see 2.3, 2.7) were labeled with Laurdan solution (final concentration of 50 μM) or DPH (final concentration of 5 μM) under continuous mixing for 4 h at 37 °C. In the case of Laurdan, an alternative way of labelling was also used [28]. Cells were incubated with a medium that contained 2 μM Laurdan for 30 min, washed and used for membrane preparation followed by SMA treatment and gel filtration fractionation (see 2.3, 2.4, 2.7).

The fluorescence spectra of Laurdan of the gel filtration fractions were recorded on an Edinburgh Instruments steady state spectrometer FS5. The emission and excitation spectra were carried out at 25 °C at 3 nm bandwidth. The emission scans were measured with the excitation wavelengths set at 340 nm, 370 nm and 410 nm; the excitation spectra were determined at the emission wavelengths set at 440 nm and 490 nm. The generalized polarization (GP) spectra were determined from the intensities of Laurdan fluorescence [29]. Specifically, the mean GP was determined as the average over the GP values in the interval of the excitation wavelength 340–390 nm according to the equation:

$$GP^{\lambda} = (I_{440} - I_{490})/(I_{440} + I_{490}),$$

where I_{490} and I_{440} represent fluorescence intensities detected at 490 nm and 440 nm, respectively, excited at excitation wavelength λ.

DPH anisotropy was monitored on a steady state spectrometer Edinburgh instruments FS5. The measurements were performed at 25 °C at 5 nm bandwidth with the excitation and emission monochromator set to 375 nm and 450 nm, respectively. The anisotropy was calculated as:

$$r_{DPH} = (I_{vv} - GI_{vh})/(I_{vv} + 2GI_{vh})$$

where I_{vv} is the fluorescence intensity measured with both excitation and emission polarized vertically and I_{vh} as the vertically polarized excitation and horizontally polarized emission. The G-factor (G) was determined by measuring a standard solution of POPOP and calculated according to:

$$G = I_{hv}/I_{hh}$$

where I_{hv} corresponds to the signal measured with the horizontally polarized excitation and vertically polarized emission and I_{hh} to the excitation and emission both polarized horizontally.

2.12. Electron microscopy

Unpurified gel filtration fractions were serially diluted (1:5, 1:25, 1:125) with lysis buffer prior to sample preparation. Fractions from density gradient ultracentrifugation were diluted 1:10. 5 μL drops of original and diluted fractions were applied onto glow discharge activated formvar/carbon-coated grids [30] and allowed to adsorb for 30 s. The excess of solution was then blotted with filter paper, and the grids were immediately negatively stained with 2% uranyl acetate in double-distilled water for 30 s. The grids were blotted again and air-dried. The samples were examined on a Philips CM100 electron microscope (Philips Eindhoven, currently Thermo Fisher Scientific) at 80 kV and at a magnification of 64,000×. Digital images were recorded at 80 kV and magnification of 56,000× using a MegaViewIII slow scan camera mounted on a FEI Morgagni electron microscope (FEI Brno, currently Thermo Fisher Scientific). The recorded images were processed in AnalySis3.2 software suite using embedded modules (Shading correction, DCE and Optimize 16-bit image for 8-bit display). No other image manipulation was used.

2.13. Lipid analysis

Sample preparation: A volume of 225 μL of cold methanol containing a mixture of lipid internal standards [PE(17:0/17:0) 900 ng; PG(17:0/17:0) 546 ng; Cer(d18:1/17:0) 225 ng, SM(d18:1/17:0) 450 ng, PC(15:0/18:1-d7) 225 ng, cholesterol-d7 2250 ng, PI(15:0/18:1-d7) 110 ng] was added to 90 μL of collected fraction and vortexed (10 s). Then, 750 μL of cold methyl *tert*-butyl ether was added, followed by vortexing (10 s) and shaking (4 °C, 6 min). Phase separation was induced by adding 130 μL of LC-MS grade water followed by centrifugation (14,000 rpm, 2 min). 350 μL of the upper organic phase was collected and evaporated. Dried lipid extracts were resuspended in 100 μL methanol containing the internal standard 12-[[(cyclohexylamino)carbonyl]amino]-dodecanoic acid (CUDA, 200 ng/mL), vortexed (10 s), and centrifuged (14,000 rpm, 2 min) prior to LC-MS analysis.

LC–MS Analysis: The LC-MS system consisted of a Vanquish UHPLC System (Thermo Fisher Scientific, Bremen, Germany) coupled to a Q

Exactive Plus mass spectrometer (Thermo Fisher Scientific). Lipids were separated on an Acquity UPLC BEH C18 column (50 × 2.1 mm; 1.7 μm) coupled to an Acquity UPLC BEH C18 VanGuard pre-column (5 × 2.1 mm; 1.7 μm) (Waters, Milford, MA, USA). The column was maintained at 65 °C at a flow-rate of 0.6 mL/min. For LC–ESI(+)-MS analysis, the mobile phase consisted of (A) 60:40 (v/v) acetonitrile:-water with ammonium formate (10 mM) and (B) 90:10:0.1 (v/v/v) isopropanol:acetonitrile:water with ammonium formate (10 mM). For LC–ESI(−)-MS analysis, the composition of the solvent mixtures were the same with the exception of the addition of ammonium acetate (10 mM) as mobile-phase modifier as previously reported [31]. Separation was conducted under the following gradient for LC–ESI(+)-MS: 0 min 15% (B); 0–1 min 30% (B); 1–1.3 min 48% (B); 1.3–5.5 min 82% (B); 5.5–5.8 min 99% (B); 5.8–6 min 99% (B); 6–6.1 min 15% (B); 6.1–7.5 min 15% (B). For LC–ESI(−)-MS, the following gradient was used: 0 min 15% (B); 0–1 min 30% (B); 1–1.3 min 48% (B); 1.3–4.8 min 76% (B); 4.8–4.9 min 99% (B); 4.9–5.3 min 99% (B); 5.3–5.4 min 15% (B); 5.4–6.8 min 15% (B). A sample volume of 5 μL was used for injection. Sample temperature was maintained at 4 °C.

The source and MS parameters were sheath gas pressure, 60 arbitrary units; aux gas flow, 25 arbitrary units; sweep gas flow, 2 arbitrary units; capillary temperature, 300 °C; aux gas heater temperature, 370 °C; MS1 mass range, *m/z* 200–1700; MS1 resolving power, 35,000 FWHM (*m/z* 200); number of data-dependent scans per cycle: 3; MS/MS resolving power, 17,500 FWHM (*m/z* 200). For ESI(+), a spray voltage of 3.6 kV and normalized collision energy of 20 and 30% was used while for ESI(−) a spray voltage of −3.0 kV and normalized collision energy of 20, 30 and 40% were set-up.

Data processing: MS-DIAL (v. 2.82) software program [32] was used for data processing. Lipids were annotated using accurate mass and MS/MS matching with LipidBlast library in MS-DIAL. In total, 260 unique lipid species covering 11 lipid classes were annotated (Supporting Table S1). Quantification was performed using class-specific internal standards [33] and expressed in pmol of particular lipid species per 1 μL of fraction. ESI(+) analysis was used for cholesterol quantification while the remaining lipids were quantified using ESI(−) data.

2.14. Detection of the GM1 glycolipid

The GM1 glycolipid membrane raft marker was detected in the gel filtration fractions (see 2.7) by dot blot method. The fractions were diluted 5× in 20 mM Tris-HCl buffer pH 8.2 containing 100 mM NaCl, and 1% SMA and 1 μL samples were applied on a strip of dry nitrocellulose. After 1 min, the strip was blocked with 5% fat-free milk solution and stained with cholera toxin-HRP conjugate.

3. Results

3.1. Disintegration of T cell membranes by SMA and properties of the raft-derived SMALPs

Cell membranes of Jurkat cells were treated with 1% SMA at room temperature for 60 min. The resulting mixture was fractionated by gel filtration on a minicolumn of Sepharose 4B. The collected fractions were analyzed by SDS PAGE and Western blotting. As shown in Fig. 1A, a vast majority of proteins were found in the low m.w. fractions which corresponding to “small” SMALPs. It is of note that only a small minority were found in the fractions corresponding to large complexes, including putative raft-derived SMALPs (membrane fragments). We suspected that some of the major membrane glycoproteins might be enriched in the fractions corresponding to large complexes but found a similar distribution was also observed for glycoproteins on blots that were stained with the lectin, concanavalin A, (Fig. 1B). A number of specific membrane proteins (LAT, PAG, Fyn, H-Ras, TCRβ, CD3ε, CD3ζ, CD5, CD18, CD45, CD71, CD147) were detectable by immunostaining of blots mostly or almost exclusively in fractions 7–9 corresponding to m.w. that were lower than 900 kDa (m.w. of IgM, which is eluted as a size standard in fractions 6–7) (Fig. 1C).

In contrast, three GPI-anchored proteins (CD48, CD55, CD59) and the protein tyrosine kinase Lck which are all considered as typical raft proteins, were partially or even mainly localized in the fractions corresponding to large SMALPs (Fig. 1C); the size distribution of these molecules was unchanged if the SMA membrane lysate was maintained at room temperature for at least 24 h before gel filtration fractionation (see below). Sonication of the fractions that contained large SMALPs resulted in the production of smaller SMALP particles (Fig. 1D).

Thus, the distribution of large SMALPs containing characteristic raft molecules (GPI-anchored proteins CD59, CD55, CD48 and protein kinase Lck) is similar to the distribution of large DRMs which were obtained after Jurkat cell membrane solubilization by detergents such as NP-40 or Brij-58 [25], while two transmembrane adaptor proteins, LAT and PAG, and partially also Fyn kinase, which are considered to be typical raft components found in DRMs [22], behaved differently and were nearly absent in the large SMALPs (Fig. 1C, E).

One of the problems associated with the use of detergents has been that DRMs, presumably derived from membrane rafts, were obtained at non-physiological low temperatures, raising the possibility that the DRMs were temperature-induced artefacts. Therefore, we performed the membrane disintegration by SMA for 1 h at 37 °C. As shown in Fig. 2, the distribution of the raft markers CD59, CD55 and Lck was also under these conditions and qualitatively similar to the distributions obtained with the samples that had been solubilized at room temperature depicted in Fig. 1. Therefore, all other experiments were done at a technically more convenient room temperature and were also more suitable for prevention of possible degradation of some proteins.

Qualitatively similar results were also obtained when, instead of isolated membranes, whole Jurkat cells were solubilized with SMA – most of the Lck, CD48, CD55 and CD59 molecules were present in fractions corresponding to large SMALPs, while the tested non-raft proteins (CD5, CD18) were present mainly in small SMALPs (Fig. 3A). Interestingly, under these circumstances Fyn, and partially also LAT and CD5 were somewhat more shifted to larger SMALPs. It may be hypothesized that under these conditions components of membrane skeleton (possibly lost during membrane preparation) may stabilize larger membrane assemblies. Similar results were also obtained with three relevant membrane proteins of murine primary T cells (Lck, Fyn, LAT) solubilized with SMA under the same conditions (Fig. 3B).

The membrane SMA lysates were alternatively fractionated by density gradient ultracentrifugation. In accordance with the results of gel filtration, the raft markers CD59, CD48 and Lck were detected mainly in the buoyant top fractions of the gradient, presumably corresponding to large SMALPs, while other tested proteins were mostly located in the bottom fractions corresponding to smaller and/or denser SMALPs (LAT, PAG, Fyn, H-Ras, TCRβ, CD3ζ). Nevertheless, minor amounts of Fyn, LAT and H-Ras were detectable also in the buoyant top fraction of the gradient (Fig. 4A).

In order to verify the relationship between the large SMALPs observed by gel filtration and those floating in the upper phase of the sucrose gradient ultracentrifugation, we subjected the combined gel filtration fractions 5 and 6 to sucrose gradient ultracentrifugation. As shown in Fig. 4B, all Lck was present in the top fractions of the gradient indicating that at least some of the large SMALPs (present in the front gel filtration fractions) correspond to the buoyant SMALPs (presumably derived from lipid-rich membrane rafts).

As expected, the large SMALPs obtained by gel filtration were quantitatively sedimented by high-speed centrifugation (Fig. 5).

We further examined whether the size distribution of SMALPs (prepared from cell membranes) containing four relevant Jurkat cell membrane molecules (Lck, Fyn, CD55, CD59) changed during prolonged incubation at room temperature. As shown in Fig. 6, distribution of the SMALPs containing these molecules remained qualitatively similar even after 24 h and did not differ much whether 1% or 3% SMA

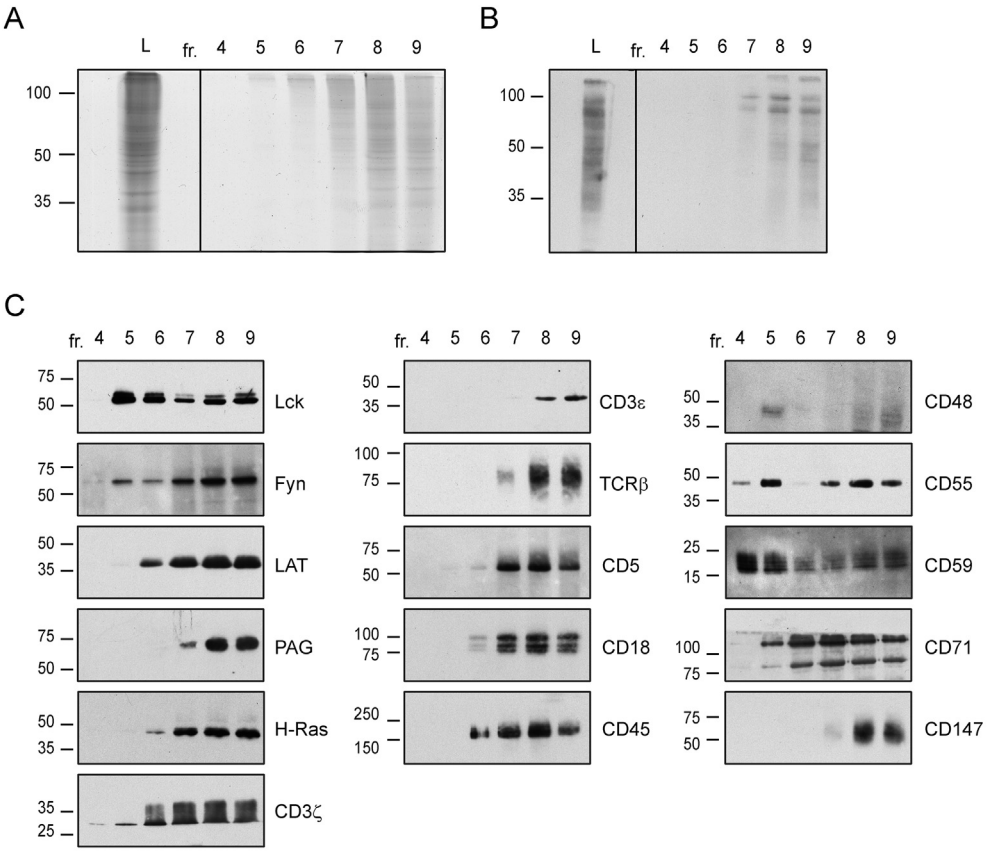

Fig. 1. Distribution of Jurkat cell membrane proteins in the gel filtration fractions. (A) The Jurkat cell membrane SMA lysate (L) was fractionated by gel filtration on a Sepharose 4B column. The fractions were analyzed by SDS PAGE on a 10% gel; proteins were stained with Coomassie Blue. (B) Depicts the same as in (A) but the glycoproteins present in the fractions were visualized after blotting with Con A – peroxidase conjugate. M.W. standard positions are indicated (in kDa). (C) Distribution of the indicated Jurkat cell membrane proteins in the fractions as detected by Western blotting; positions of m.w. standards (kDa) are indicated. (D) The effect of SMA lysate sonication on the distribution of the indicated Jurkat cell membrane proteins in the fractions. (E) Comparison of the distribution of the two indicated Jurkat cell membrane proteins in the fractions of membranes lysed by two indicated detergents and SMA.

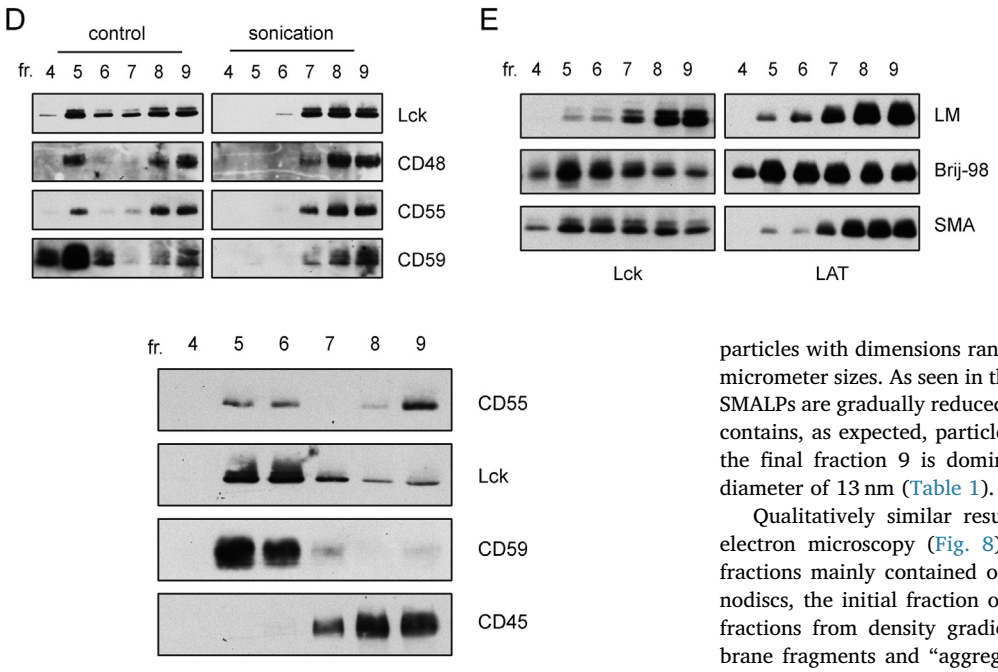

Fig. 2. Gel filtration of Jurkat cell membranes solubilized by SMA at 37 °C. The indicated Jurkat cell membrane proteins were detected in the Sepharose 4B gel filtration by Western blotting. For other details see legend to Fig. 1.

was used. Reduced intensity of the zones in fractions 7–9 in the samples incubated for 24 h may be due to partial protein degradation.

In order to obtain more detailed information regarding the size composition of the SMA solubilized Jurkat cell membrane gel filtration fractions, we examined the fractions by dynamic light scattering (DLS) (Fig. 7). The unfractionated sample (upper panel) appears to contain particles with dimensions ranging from a few nanometers up to almost micrometer sizes. As seen in the bottom panels of Fig. 7, the sizes of the SMALPs are gradually reduced in the Sepharose 4B fractions. Fraction 4 contains, as expected, particles in the range of hundreds of nm, while the final fraction 9 is dominated by components bearing the mean diameter of 13 nm (Table 1).

Qualitatively similar results were also obtained by transmission electron microscopy (Fig. 8) – while the "low m.w." gel filtration fractions mainly contained objects of expected shape and size of nanodiscs, the initial fraction of the Sepharose 4B column (and the top fractions from density gradient ultracentrifugation) contained membrane fragments and "aggregates" of the size corresponding to those detected by DLS.

3.2. Lipid composition of SMALPs

As our results indicated, the large Jurkat cell membrane SMALPs might be derived from membrane rafts (due to the presence of several typical raft protein markers), hence we also analyzed by liquid chromatography–mass spectrometry (LC–MS) the lipid composition of the fractions obtained by gel filtration. As shown in Fig. 9, there were distinct differences between the large and small SMALPs, present in gel

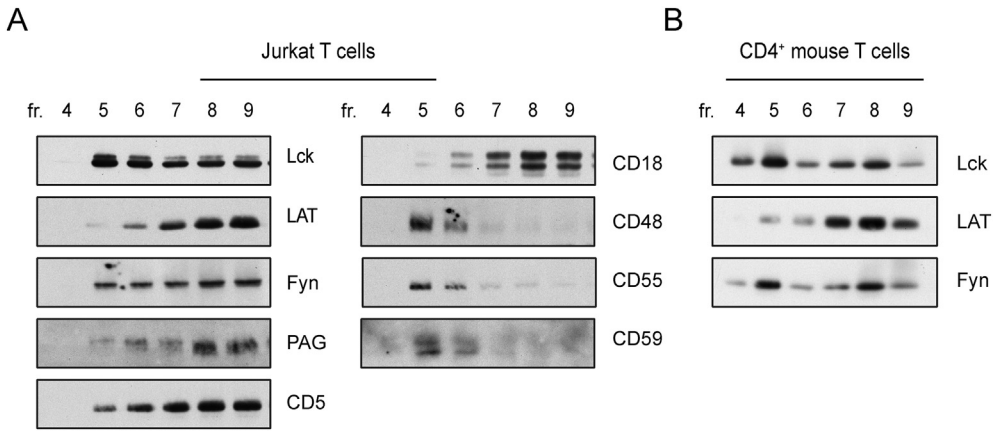

Fig. 3. Distribution of Jurkat cell membrane proteins in the gel filtration fractions. (A) Whole Jurkat cells were solubilized with SMA, lysate fractionated by gel filtration and analyzed as in Fig. 1C. (B) Depicts the same as in (A) but using murine primary T cells.

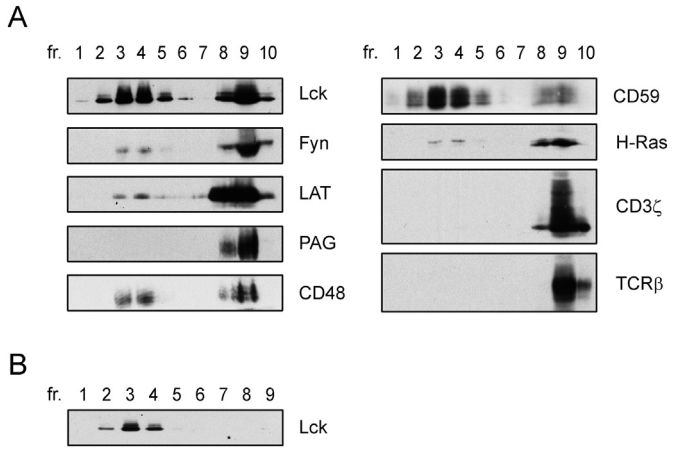

Fig. 4. Distribution of Jurkat cell membrane proteins in the density gradient ultracentrifugation. (A) The Jurkat cell membrane SMA lysate was fractionated by density gradient ultracentrifugation and the indicated proteins in the fractions were detected by Western blotting; fr. 10 is sediment. (B) Combined gel filtration fractions 5 and 6 (containing large SMALPs) were subjected to sucrose gradient ultracentrifugation. The distribution of Lck was determined by Western blotting. As described in paragraph 2.5., the fractions contained approximately the following percentage of sucrose: 2 (5%), 3 (10%), 4 (20%), 5 (25%), 6 (30%), 7 (30%), 8 (35%), 9 (40%).

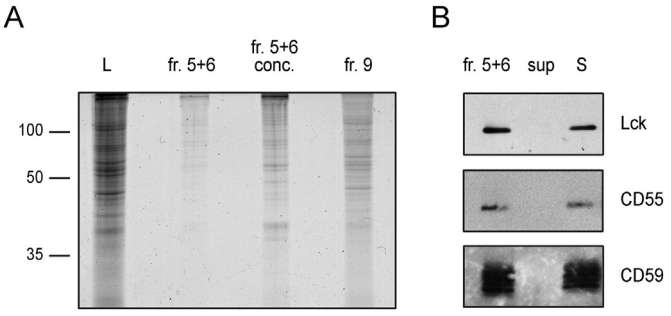

Fig. 5. Sedimentation of large raft-derived SMALPs by ultracentrifugation. Jurkat cell membranes were disintegrated with SMA, fractionated by gel filtration on Sepharose 4B. SMALPs present in fractions 5 and 6 were subjected to ultracentrifugation. (A) SDS PAGE of the indicated samples – whole membrane SMA lysate (L), combined fractions 5 + 6, fractions 5 + 6 concentrated 10× by ultracentrifugation, combined fractions 8 + 9; stained with Coomassie Blue (comparison of proteins present in the large and small SMALPs). M.W. (in kDa) standard positions are indicated. (B) Western blotting of raft molecules Lck, CD55 and CD59 following ultracentrifugation of gel filtration fractions 5 + 6 (combined fractions 5 + 6, supernatant after ultracentrifugation (sup), sediment adjusted to original volume (S)).

filtration fractions 5, 6 and fraction 9, respectively; the former were enriched in cholesterol, phosphatidylserines (PS), sphingomyelins (SM), ceramides (Cer) and monohexosylceramides (HexCer) while in the latter phosphatidylcholines (PC), phosphatidylethanolamines (PE), etherPC/etherPE (ether-linked species of PC/PE), phosphatidylinositols (PI) and phosphatidylglycerols (PG) were prevalent (Fig. 9A). The lipids present in fraction 5 contained markedly more saturated fatty acids and just little of those containing multiple double bonds, as shown in Fig. 9B on phosphatidylcholines (PC). Furthermore, only the large SMALPs contained the glycosphingolipid GM1 as detected by cholera toxin binding (Fig. 9C). These results correspond to the assumption that the large SMALPs may be indeed derived from membrane rafts.

The raft origin of Jurkat cell membrane large SMALPs is also supported by the results from experiments with lipid probes sensitive to lipid membrane fluidity (membrane order). As demonstrated in Fig. 10, the lipid environment in large SMALPs appears to be less fluid than in the small ones, which may indicate the presence of a more ordered lipid L_o phase which is characteristic of membrane rafts [34]. Furthermore, the specific presence of the GM1 glycosphingolipid in the fractions containing large SMALPs (Fig. 9C) is also consistent with their possible raft origin.

Results qualitatively similar to those obtained with the Laurdan probe were also obtained when using the lipid probe 1,6-diphenylhexatriene (DPH). This hydrophobic dye penetrates deeper in the membrane interior in comparison to Laurdan and is sensitive to lipid ordering within the fatty acid region [38]. As apparent from the higher values of DPH anisotropy (Fig. 11); gel filtration fractions 4–6 which contain large SMALPs appeared to include more ordered (less fluid) lipid environment than those containing small SMALPs.

3.3. Immunoprecipitation of SMA-solubilized membrane proteins

If the use of SMA is really an equivalent or better alternative to currently used detergents, then it should be possible to readily immunoprecipitate membrane proteins and their complexes solubilized by SMA, just as it is possible after solubilization with commonly used detergents. Indeed, as shown in Fig. 12A, immunoprecipitation works well for several tested T cell surface proteins (CD18, LAT, Fyn).

When the Sepharose 4B fractions corresponding to large SMALPs were used for the immunoprecipitation of Lck, the recovery of the immunoisolated protein was very low, which was probably due to the large size of the SMALPs that were unable to penetrate into the Protein

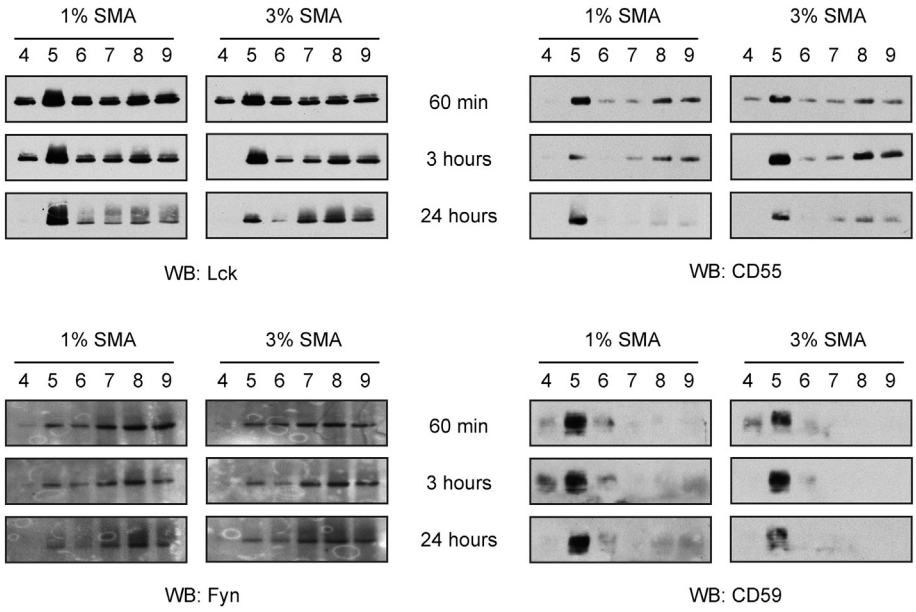

Fig. 6. Stability of SMAPLs and effects of SMA concentration. Jurkat cell membranes were solubilized by 1% or 3% SMA, fractionated by gel filtration on Sepharose 4B and the fractions were examined by SDS PAGE/Western blotting after the indicated time periods.

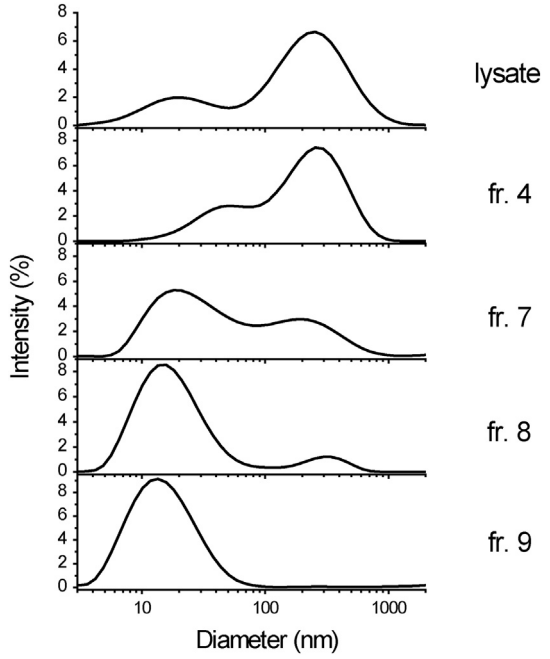

Fig. 7. Intensity weighted distributions of the selected fractions obtained by dynamic light scattering (DLS). The panels depict the distribution of SMALPs in the indicated samples (before fractionation and in the indicated Sepharose 4B column fractions). Importantly, the intensity signal (referred to as Intensity (%)) is not directly proportional to the number of respective components since the scattering intensity depends on the sixth power of the particle size. As a consequence, the distribution is strongly biased towards the larger species while suppressing the smaller particles. Therefore, in absolute numbers the particles with dimensions on the order of 10 nm are much more abundant in the unfractionated sample than the (sub)micrometer sample.

A/G Sepharose 4B beads (not shown). However, recovery of the immunoprecipitated protein was improved when the large SMALPs were disintegrated by sonication before immuno-isolation (Fig. 12B).

Table 1
Parameters set in accordance to the intensity weighted distribution functions recorded for various fractions. The distributions were fitted with two Gaussian curves yielding the following parameters: position of fitted peaks (r_i), respective full widths at half maxima ($FWHM_i$), and their individual relative percentual contributions to the overall distribution (Int_i).

Fraction	r_1 (nm)	$FWHM_1$ (nm)	Int_1	r_2 (nm)	$FWHM_2$ (nm)	Int_2
4	295	311	78	106	42	22
5	302	324	59	101	39	41
6	277	284	31	78	34	69
7	324	304	14	56	27	86
8	72	63	42	18	17	58
9	81	71	11	13	16	89

4. Discussion

4.1. SMA as a potentially optimal alternative to commonly used detergents

Previous studies have shown that membrane fragments (nanodiscs) produced by exposure to the styrene-maleic acid (SMA) amphipathic copolymer probably preserve the native lipid environment around membrane proteins [14,15,39,40]. Therefore, the primary aim of this study was to verify whether SMA can be used instead of commonly used mild detergents for disintegration of T cell membranes and for biochemical studies on T cell membrane proteins.

Our results on a number of T cell membrane proteins demonstrate that SMA indeed is, in this respect, comparable to detergents such as octylglucoside or Triton X-100 (efficient solubilization, compatibility with Western blotting and immunoprecipitation) that are currently used. One drawback regarding the activity of SMA is that (in contrast to most commonly used mild detergents) it disrupts nuclear membranes, so it is necessary to digest the released viscous DNA (see also [41]). Solubilization of whole cells obviously has some advantages (much simpler, minimal amounts of cells are sufficient, a decrease in potential artefacts due to the breaking of associations with the membrane skeleton).

It is still possible that lipid rearrangements occur even during SMA mediated membrane disintegration, but these may be less severe than in the case of DRMs. Obviously, the degree of correspondence of the lipid environment within the SMALP nanodiscs vs. the native membrane is

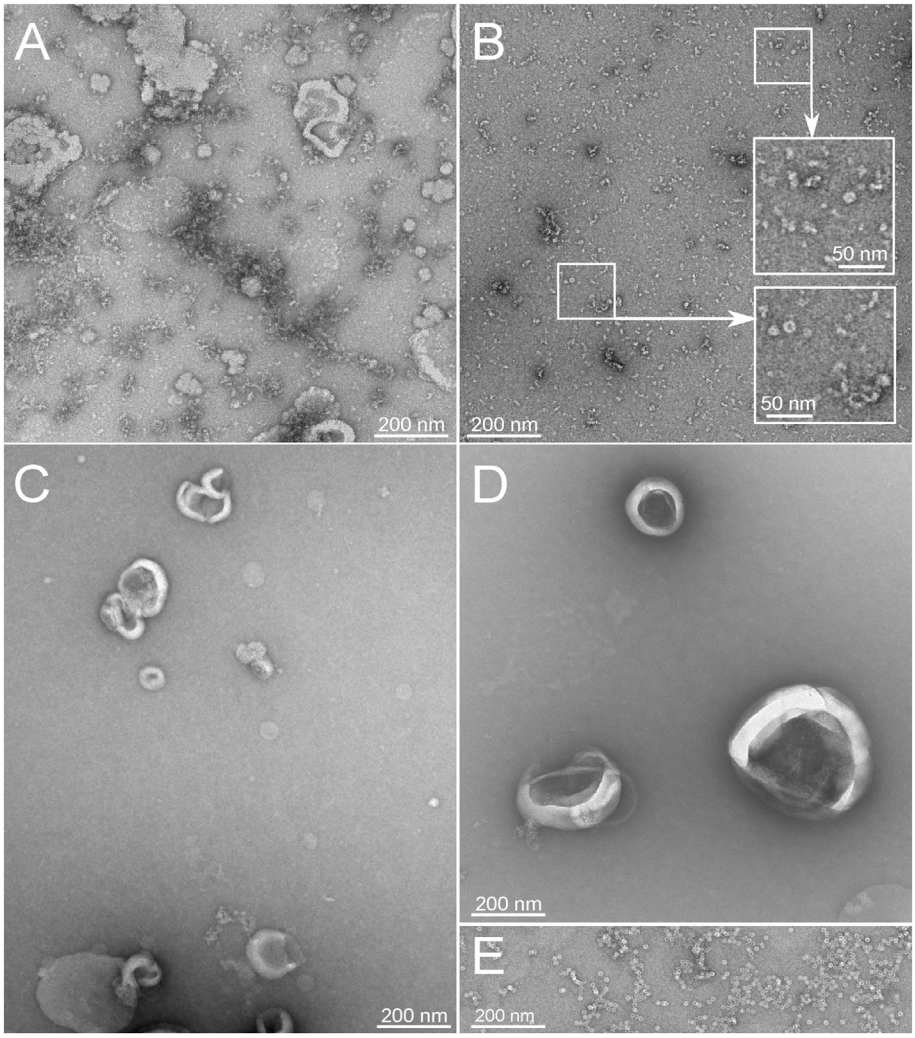

Fig. 8. Transmission electron microscopy. Negative staining of gel chromatography fractions. (A) A representative image of the population of particles in the pooled undiluted fractions 5 + 6, showing membrane fragments and large aggregates. (B) A representative image of the population of particles in the pooled fractions 8 + 9, diluted 1:25. The size of the imaged particles reflects data from DLS for fractions 8 and 9 (Fig. 7). (C) and (D) Representative images of particles in fractions 3 and 4, respectively, from density gradient ultracentrifugation (those from Fig. 4B). (E) Horse spleen ferritin particles used as an external standard, concentration 100 μg/mL.

an important issue of further investigation. Nevertheless, we believe that SMA may be a useful tool for examination of more or less specific associations of various leukocyte receptors and other membrane molecules with specific lipids, and their changes upon activation or ligand engagement.

4.2. SMA as a tool for biochemical studies on membrane rafts

Furthermore, we wondered whether SMA could be used for the preparation of biochemical equivalents of T cell membrane rafts, which might be much closer to native rafts than the previously widely studied (and later criticized) detergent-resistant membrane fragments (DRMs).

As the presently prevailing view of native membrane rafts is that they are very small, highly dynamic nanodomains that are under 20 nm in size [1], we expected that SMA-based disintegration of the T lymphocyte membrane would result in similarly small-sized, raft-derived nanodiscs (SMALPs) containing proteins that are typically associated with rafts (GPI-anchored ones, Src-family kinases, Ras family G-proteins, palmitoylated transmembrane adaptor proteins). This expectation was fulfilled for some of these proteins (LAT, PAG, H-Ras) but somewhat surprisingly, relatively large fractions of GPI-anchored proteins (CD48, CD55, CD59) and Src family kinase Lck (and less prominently Fyn) were found in much larger buoyant membrane fragments, as detected by gel filtration and density gradient ultracentrifugation. The size of the small and large SMALPs separated by Sepharose 4B gel filtration was confirmed by dynamic light scattering (Fig. 7) and electron microscopy (Fig. 8).

These large SMALPs thus resembled the large DRMs that have been produced by detergents such as NP-40 or Brij-58 in previous studies [25] [42]. There was an obvious possibility that the large SMALPs were artefacts due to the non-physiological temperature used during membrane disintegration. Importantly, essentially the same results were obtained when membrane solubilization was performed at 37 °C (Fig. 2).

Of course, we cannot exclude the possibility that SMA somehow induces aggregation of specific lipids (those containing mostly saturated fatty acid chains, cholesterol) and specific lipidated proteins (GPI-anchored and myristoylated and palmitoylated Src-family kinases).

Nevertheless, we speculate that there may be several types of membrane rafts which differ in their sensitivity to disintegration by SMA or by their intrinsic tendency to aggregate into larger patches. Thus, those containing the GPI-anchored proteins and Src-family kinases may differ from those containing palmitoylated transmembrane adaptor proteins (LAT, PAG) or Ras family proteins.

The idea that the large, buoyant SMALPs contain several GPI-anchored proteins and Src-family kinases may be derived from membrane

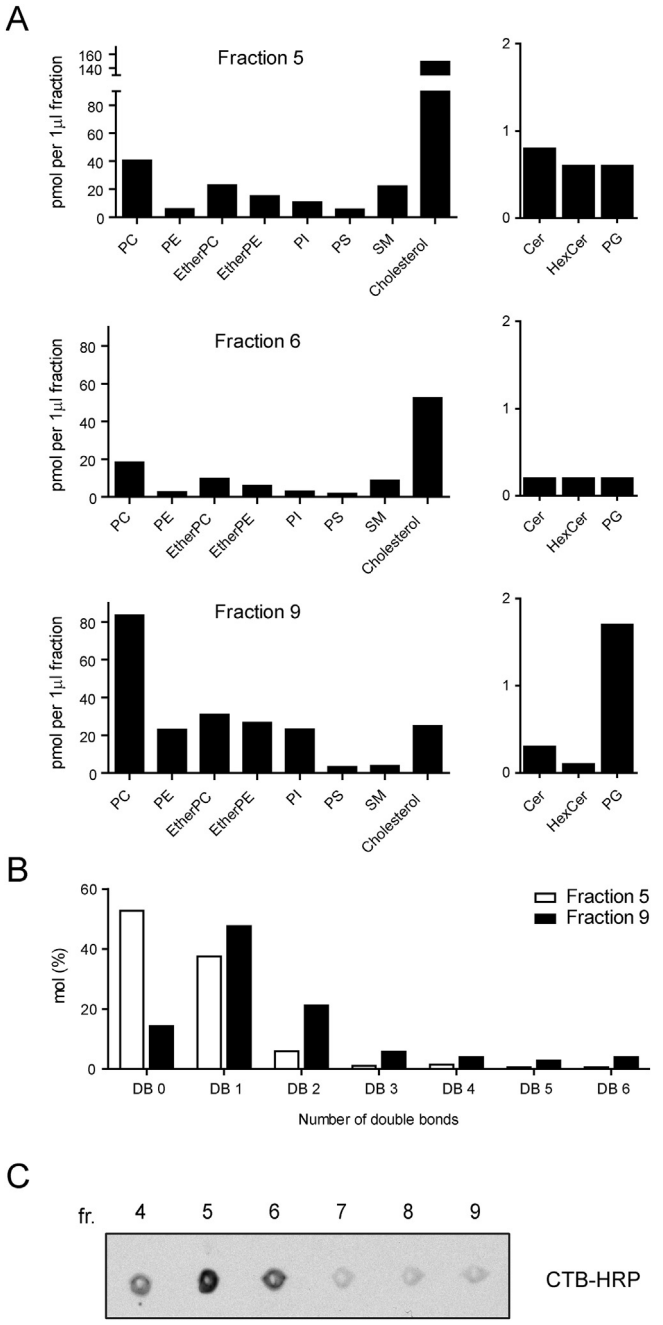

Fig. 9. Lipid composition of gel filtration fractions. (A) Distribution of lipid classes across fractions 5, 6 and 9, (B) molar percentage of total PC species based on number of double bonds (DB) across fractions 5 and 9. (Legend: Cer, ceramides; HexCer, monohexosylceramides; EtherPC, ether-linked phosphatidylcholines; EtherPE, ether-linked phosphatidylethanolamines; PC, phosphatidylcholines; PE, phosphatidylethanolamines; PG, phosphatidylglycerols; PI, phosphatidylinositols; PS, phosphatidylserines; SM, sphingomyelins) (C) Dot blot detection of GM1 glycolipid in the respective gel filtration fractions (staining with cholera toxin-HRP conjugate).

rafts is supported by our lipidomics analysis (paragraph 3.2., Fig. 9) and experiments which have been based on the use of lipid probes (Laurdan and DPH) sensitive to the properties of their lipidic environment (Figs. 10 and 11).

At the moment, it is unclear whether the components of the large SMALPs reside jointly in common membrane patches or if several types of such entities exist. Also, we do not know at this moment whether the large, raft-derived SMALPs that we have observed have a structure that is similar to the small ones, i.e. whether they also have a belt of SMA molecules around their rim.

We certainly do not claim that everything present in fractions 4–6 of Sepharose 4B gel filtration more or less corresponds to membrane rafts. Future research should elucidate the heterogeneity of these large, SMA-resistant entities. We are currently working on a proteomic and lipidomic study characterizing the various subfractions of this material. Nevertheless, the results shown in Fig. 4B demonstrate that at least the large SMALPs containing Lck rather uniformly float in density gradient ultracentrifugation (i.e. apparently no large dense Lck-containing SMALPs exist). On the other hand, the bottom fractions of the density gradient most likely contain a complex mixture of large dense complexes as well as various small entities of various densities. Ultracentrifugation at higher speeds might achieve separation of these molecular complexes.

Our results may indicate that previous membrane raft studies that employed mild detergents and DRMs may not be largely artefactual, but possibly do reflect important specific features of raft membrane nanodomains. Just as in the case of the previous detergent-based results, our data demonstrate that certain percentages of raft molecules (GPI-anchored glycoproteins, Src-family kinases) were fully solubilized with SMA and present in small SMALPs. This may indicate that these molecules undergo dynamic exchange between raft and non-raft areas of the membrane (the result from the use of a detergent or SMA solubilization represents a “snapshot” of the actual state). Another possibility is that membrane rafts of various sizes may co-exist in the membranes. In future experiments, it will be interesting to compare the lipid and protein composition of the SMALPs of different sizes and determine their possible relationship (e.g. the small ones corresponding to “elementary nanorafts”, while the larger ones being their aggregates).

As stated above, another class of presumably raft-associated membrane proteins, namely palmitoylated transmembrane adaptors, represented here by LAT and PAG, were more fully solubilized by SMA than in previous studies by polyoxyethylene detergents [26,43], and were present almost entirely in small SMALPs. Furthermore, Fyn kinase behaved differently from Lck, as only its relatively minor fraction was detectable in the large SMALPs of Jurkat cell membranes. Interestingly, this difference was more prominent when SMALPs were prepared from isolated membranes; when prepared directly from whole T cells, size distributions of SMALPs containing Lck or Fyn were similar (Fig. 3). Nevertheless, this difference between Lck and Fyn (perhaps due to their differential interactions with membrane skeleton components) may be relevant for their well-established functional differences [44]. It is possible that some non-raft proteins, such as CD71 (cf. Fig. 1C), can be present in so far uncharacterized type of membrane microdomains yielding intermediate to large SMALPs. This will also be an interesting subject of further studies.

4.3. Technical aspects

It should be noted that gel filtration on Sepharose 4B used as a basic method in this study has low resolving power. It separates well the small SMALPs (around 20 nm) from the large ones (hundreds of nm) but optimized gel media should be used in future experiments for separation of various SMALP species in both these fractions.

As stated above, the results of membrane disintegration by SMA at physiological temperature appear to be similar to those at room temperature (Fig. 2), indicating that temperature artefacts may not be a problem. Furthermore, large SMALPs appear to be relatively stable during prolonged incubation with excess SMA at ambient temperature (Fig. 6). Nevertheless, their exposure to 3% SMA at ambient temperature for 24 h resulted in their partial dissociation or degradation of some of their components (Fig. 6). On the other hand, protein degradation should be limited because of the presence of a mixture of protease inhibitors in the lysis buffer.

Finally, an important technical aspect is reproducibility of the

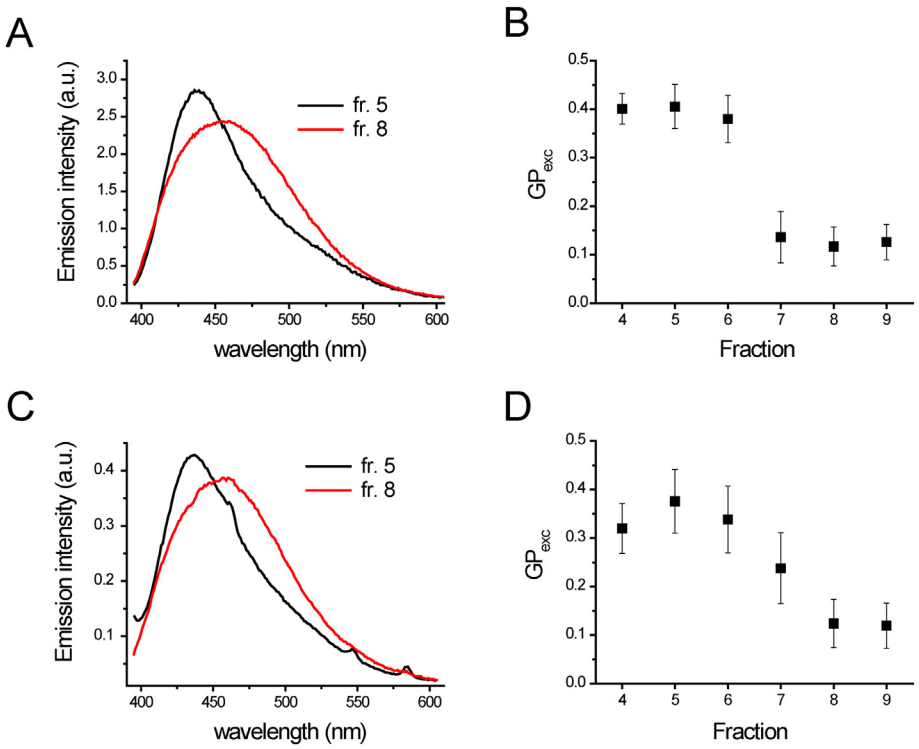

Fig. 10. Examination of lipid order in SMALPs present in gel filtration fractions using Laurdan. (A, B) Jurkat cell membranes were disintegrated with SMA, subsequently separated by gel filtration on Sepharose 4B and ultimately incubated with Laurdan. (A) Emission spectra of Laurdan in fractions 5 and 8. The emission spectrum of fraction 5 exhibits a maximum at 435 nm. The emission spectra of Laurdan embedded in rigid lipid phases are known to have a maximum of approximately 440 nm [35] [36]; thus, the result indicates the presence of the Laurdan probe in a relatively rigid and ordered lipid environment. In contrast, the emission spectrum of fraction 8 was significantly shifted to the longer wavelength, indicating the presence of the Laurdan probe in a more disordered (fluid) lipid environment. (B) Laurdan generalized polarization (GP). The generalized polarization (GP_{exc}) values confirmed the conclusions made from the inspection of the steady state spectra: the higher GP_{exc} values in fractions 4–6 indicated the presence of the Laurdan probe in a relatively more ordered lipid environment as compared to fractions 7–9. In order to correlate the presently recorded GP_{exc} values to the previous data obtained for model membranes [37], GP_{exc} of fractions 4–6 corresponds to the model phospholipid bilayer with prevailing liquid ordered phase (e.g. POPC/egg sphingomyelin/Cholesterol = 25:35:40 at 20 °C), while fractions 7–9 correspond to the model bilayers with predominant liquid disordered phase (e.g. POPC/egg sphingomyelin/Cholesterol = 70:25:5 at 20 °C) [37]. (C, D) report the same as in (A, B) but using samples of fractions obtained from membranes prepared from whole Jurkat cells incubated first with Laurdan and subsequently disintegrated by SMA and separated by gel filtration (see paragraph 2.11.).

results. Obviously, when comparing gel filtration results from different experiments, there are relatively minor differences in relative distributions of the raft-associated proteins (Lck, Fyn, CD48, CD55, CD59) in the large vs. small SMALPs (cf. Figs. 1C, D, E, 6). This variability may be due to both intrinsic and technical factors. The intrinsic factors may include differences in cell culture density and presence of small cell aggregates. Different batches of membrane preparations may somewhat differ in the contents of intracellular membranes (containing different forms of the relevant molecules, such as underglycosylated ones), the volumes of manually collected fractions from the Sepharose 4B minicolums may differ by ca 10%, there may be minor differences in Western blotting transfer efficiency and antibody staining. When performed with an identical starting cell culture, the results of 3 parallel experiments are very similar (Fig. 13).

In conclusion, we hypothesize that SMA (or similar copolymers [45]) may be the long sought optimal tools of membrane biochemistry making it possible to study also membrane molecules of immunocytes and their associations under more natural conditions than when using various detergents, namely in the case of raft-associated molecules. Future studies should confirm or disprove such a working hypothesis.

Supplementary data to this article can be found online at https://doi.org/10.1016/j.bbamem.2018.08.006.

Author contributions

P.A. and V.H. designed research, P.A., O.B. O.B., D.P., J.P., T.C. and J.S. performed research, V.H. wrote the manuscript that was edited by all authors.

Transparency document

The Transparency document associated with this article can be found, in online version.

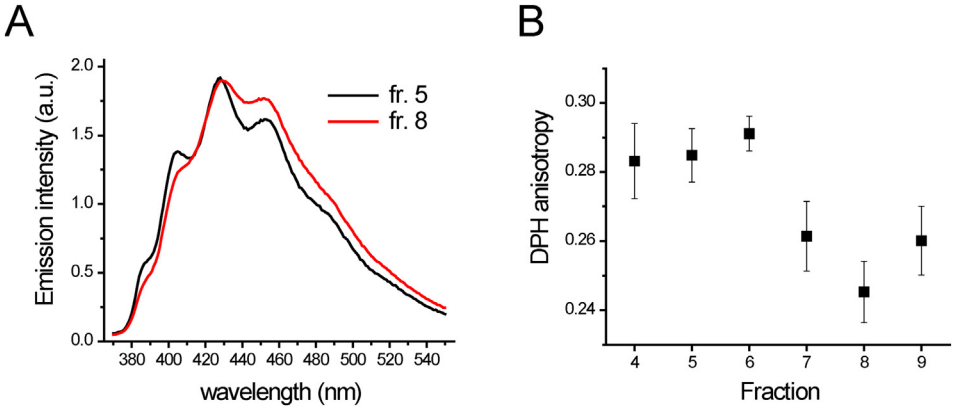

Fig. 11. Examination of lipid order in SMALPs present in gel filtration fractions using DPH. As in Fig. 10 A, B, but using the DPH probe (for details see paragraph 2.11.).

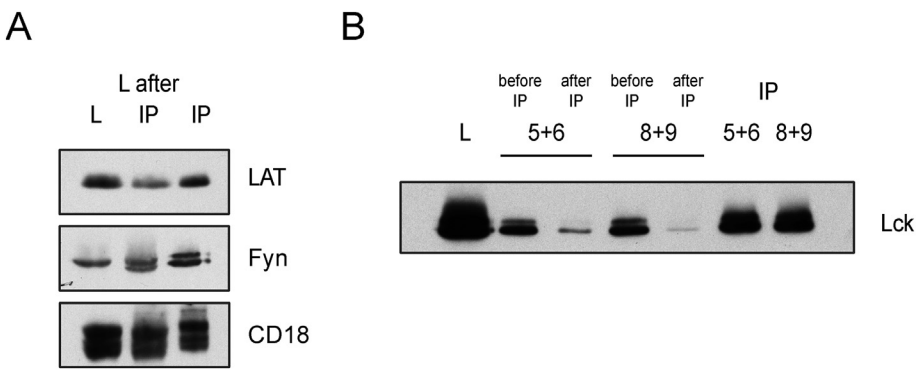

Fig. 12. Immunoprecipitation of membrane proteins solubilized by SMA. (A) The indicated proteins were immunoisolated from a Jurkat cell membrane SMA lysate (L) and immunoprecipitates (IP) were analyzed by SDS PAGE followed by Western blotting. "L after IP" represents supernatant after IP. The double band in the Fyn samples may be due to changes in phosphorylation induced during the IP procedure; the multiple bands in the CD18 samples likely correspond to various partially glycosylated forms that are found in intracellular and plasma membranes. (B) Jurkat cell membranes were solubilized with SMA, fractionated by gel filtration on Sepharose 4B and sonicated. Lck was immunoisolated from combined sonicated fractions 5 + 6 (corresponding to large SMALPs) or the combined fractions 8 + 9 (corresponding to small nanodiscs).

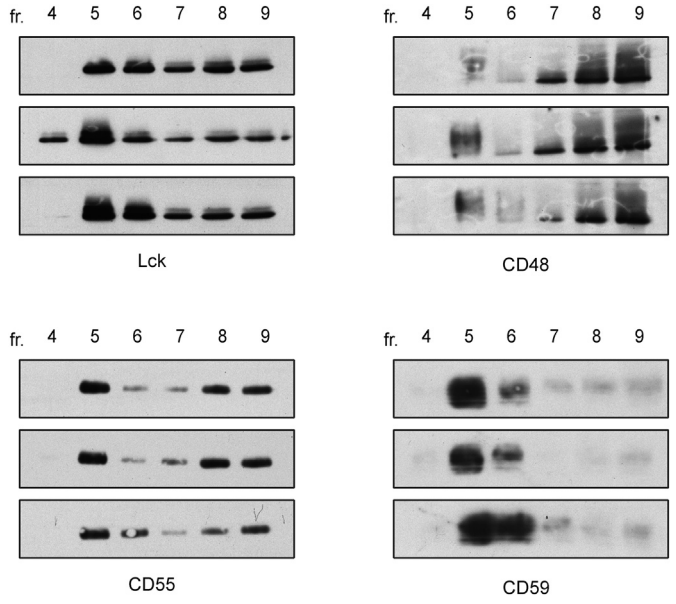

Fig. 13. Reproducibility of gel filtration results. Three batches of cell membranes were separately prepared from a common Jurkat cell culture and used for SMA disintegration, separation by gel filtration on Sepharose 4B (see paragraphs 2.3, 2.4., 2.7), SDS PAGE and Western blotting.

Acknowledgements

We thank all antibody donors, Dr. Stefan Scheidelaar for his expert consultation, and Zuzana Dolejsi for electron microscopic analysis of the samples. This work was supported by Grant No. P302-12-G101 from the Czech Science Foundation and by the Institute of Molecular Genetics of the Czech Academy of Sciences (RVO 68378050). O. Benada is supported by project LO1509 (Ministry of Education, Youth and Sports (MEYS) of the Czech Republic). Jan Sykora acknowledges the Czech Science Foundation via 17-05903S.

T. Cajka was supported by Institute of Physiology of the Czech Academy of Sciences (RVO:67985823). The Microscopy Centre - Electron Microscopy CF, IMG AS CR is supported by the Czech-BioImaging large RI project (LM2015062 funded by MEYS CR) and by OP RDE (CZ.02.1.01/0.0/0.0/16_013/0001775 "Modernization and support of research activities of the national infrastructure for biological and medical imaging Czech-BioImaging"). The language correction by Jasper Manning is gratefully appreciated.

References

[1] E. Sezgin, I. Levental, S. Mayor, C. Eggeling, The mystery of membrane organization: composition, regulation and roles of lipid rafts, Nat. Rev. Mol. Cell Biol. 18 (2017) 361–374.

[2] D.A. Brown, J.K. Rose, Sorting of GPI-anchored proteins to glycolipid-enriched membrane subdomains during transport to the apical cell surface, Cell 68 (1992) 533–544.

[3] K. Fiedler, T. Kobayashi, T.V. Kurzchalia, K. Simons, Glycosphingolipid-enriched, detergent-insoluble complexes in protein sorting in epithelial cells, Biochemistry 32 (1993) 6365–6373.

[4] S.N. Ahmed, D.A. Brown, E. London, On the origin of sphingolipid/cholesterol-rich detergent-insoluble cell membranes: physiological concentrations of cholesterol and sphingolipid induce formation of a detergent-insoluble, liquid-ordered lipid phase in model membranes, Biochemistry 36 (1997) 10944–10953.

[5] S. Ilangumaran, D.C. Hoessli, Effects of cholesterol depletion by cyclodextrin on the sphingolipid microdomains of the plasma membrane, Biochem. J. 335 (1998) 433–440.

[6] T.M. Stulnig, M. Berger, T. Sigmund, D. Raederstorff, H. Stockinger, W. Waldhausl, Polyunsaturated fatty acids inhibit T cell signal transduction by modification of detergent-insoluble membrane domains, J. Cell Biol. 143 (1998) 637–644.

[7] H. Heerklotz, Triton promotes domain formation in lipid raft mixtures, Biophys. J. 83 (2002) 2693–2701.

[8] S. Schuck, M. Honsho, K. Ekroos, A. Shevchenko, K. Simons, Resistance of cell membranes to different detergents, Proc. Natl. Acad. Sci. U. S. A. 100 (2003) 5795–5800.

[9] E. Sevcsik, G.J. Schutz, With or without rafts? Alternative views on cell membranes, BioEssays 38 (2016) 129–139.

[10] I. Levental, M. Grzybek, K. Simons, Raft domains of variable properties and compositions in plasma membrane vesicles, Proc. Natl. Acad. Sci. U. S. A. 108 (2011) 11411–11416.

[11] T.J. Knowles, R. Finka, C. Smith, Y.P. Lin, T. Dafforn, M. Overduin, Membrane proteins solubilized intact in lipid containing nanoparticles bounded by styrene maleic acid copolymer, J. Am. Chem. Soc. 131 (2009) 7484–7485.

[12] J.M. Dorr, S. Scheidelaar, M.C. Koorengevel, J.J. Dominguez, M. Schafer, C.A. van Walree, J.A. Killian, The styrene-maleic acid copolymer: a versatile tool in membrane research, Eur. Biophys. J. 45 (2016) 3–21.

[13] M. Jamshad, J. Charlton, Y.P. Lin, S.J. Routledge, Z. Bawa, T.J. Knowles, M. Overduin, N. Dekker, T.R. Dafforn, R.M. Bill, D.R. Poyner, M. Wheatley, G-protein coupled receptor solubilization and purification for biophysical analysis and functional studies, in the total absence of detergent, Biosci. Rep. 35 (2015).

[14] M. Jamshad, Y.P. Lin, T.J. Knowles, R.A. Parslow, C. Harris, M. Wheatley, D.R. Poyner, R.M. Bill, O.R. Thomas, M. Overduin, T.R. Dafforn, Surfactant-free purification of membrane proteins with intact native membrane environment, Biochem. Soc. Trans. 39 (2011) 813–818.

[15] M. Jamshad, V. Grimard, I. Idini, T.J. Knowles, M.R. Dowle, N. Schofield, P. Sridhar, Y.P. Lin, R. Finka, M. Wheatley, O.R.T. Thomas, R.E. Palmer, M. Overduin, C. Govaerts, J.M. Ruysschaert, K.J. Edler, T.R. Dafforn, Structural analysis of a nanoparticle containing a lipid bilayer used for detergent-free extraction of membrane proteins, Nano Res. 8 (2015) 774–789.

[16] C. Logez, M. Damian, C. Legros, C. Dupre, M. Guery, S. Mary, R. Wagner, C. M'Kadmi, O. Nosjean, B. Fould, J. Marie, J.A. Fehrentz, J. Martinez, G. Ferry, J.A. Boutin, J.L. Baneres, Detergent-free isolation of functional G protein-coupled receptors into nanometric lipid particles, Biochemistry 55 (2016) 38–48.

[17] S. Gulati, M. Jamshad, T.J. Knowles, K.A. Morrison, R. Downing, N. Cant, R. Collins, J.B. Koenderink, R.C. Ford, M. Overduin, I.D. Kerr, T.R. Dafforn, A.J. Rothnie, Detergent-free purification of ABC (ATP-binding-cassette) transporters, Biochem. J. 461 (2014) 269–278.

[18] D.J. Swainsbury, S. Scheidelaar, R. van Grondelle, J.A. Killian, M.R. Jones, Bacterial reaction centers purified with styrene maleic acid copolymer retain native membrane functional properties and display enhanced stability, Angew. Chem. Int. Ed. Eng. 53 (2014) 11803–11807.

[19] A.J. Bell, L.K. Frankel, T.M. Bricker, High yield non-detergent isolation of photosystem I-light-harvesting chlorophyll II membranes from spinach thylakoids: IMPLICATIONS FOR THE ORGANIZATION OF THE PS I ANTENNAE IN HIGHER PLANTS, J. Biol. Chem. 290 (2015) 18429–18437.

[20] I.A. Smirnova, D. Sjostrand, F. Li, M. Bjorck, J. Schafer, H. Ostbye, M. Hogbom, C. von Ballmoos, G.C. Lander, P. Adelroth, P. Brzezinski, Isolation of yeast complex IV in native lipid nanodiscs, BBA-Biomembranes 1858 (2016) 2984–2992.

[21] I. Stefanova, V. Horejsi, I.J. Ansotegui, W. Knapp, H. Stockinger, GPI-anchored cell-

surface molecules complexed to protein tyrosine kinases, Science 254 (1991) 1016–1019.
[22] V. Horejsi, M. Hrdinka, Membrane microdomains in immunoreceptor signaling, FEBS Lett. 588 (2014) 2392–2397.
[23] Y.J. Jin, M.W. Albers, W.S. Lane, B.E. Bierer, S.L. Schreiber, S.J. Burakoff, Molecular cloning of a membrane-associated human FK506- and rapamycin-binding protein, FKBP-13, Proc. Natl. Acad. Sci. U. S. A. 88 (1991) 6677–6681.
[24] P. Otahal, P. Angelisova, M. Hrdinka, T. Brdicka, P. Novak, K. Drbal, V. Horejsi, A new type of membrane raft-like microdomains and their possible involvement in TCR signaling, J. Immunol. 184 (2010) 3689–3696.
[25] T. Cinek, V. Horejsi, The nature of large noncovalent complexes containing glycosyl-phosphatidylinositol-anchored membrane glycoproteins and protein tyrosine kinases, J. Immunol. 149 (1992) 2262–2270.
[26] T. Brdicka, D. Pavlistova, A. Leo, E. Bruyns, V. Korinek, P. Angelisova, J. Scherer, A. Shevchenko, I. Hilgert, J. Cerny, K. Drbal, Y. Kuramitsu, B. Kornacker, V. Horejsi, B. Schraven, Phosphoprotein associated with glycosphingolipid-enriched microdomains (PAG), a novel ubiquitously expressed transmembrane adaptor protein, binds the protein tyrosine kinase csk and is involved in regulation of T cell activation, J. Exp. Med. 191 (2000) 1591–1604.
[27] J. Brejchova, J. Sykora, K. Dlouha, L. Roubalova, P. Ostasov, M. Vosahlikova, M. Hof, P. Svoboda, Fluorescence spectroscopy studies of HEK293 cells expressing DOR-G(i)1 alpha fusion protein; the effect of cholesterol depletion, BBA-Biomembranes 1808 (2011) 2819–2829.
[28] O. Golfetto, E. Hinde, E. Gratton, Laurdan fluorescence lifetime discriminates cholesterol content from changes in fluidity in living cell membranes, Biophys. J. 104 (2013) 1238–1247.
[29] M. Amaro, R. Sachl, P. Jurkiewicz, A. Coutinho, M. Prieto, M. Hof, Time-resolved fluorescence in lipid bilayers: selected applications and advantages over steady state, Biophys. J. 107 (2014) 2751–2760.
[30] O. Benada, V. Pokorny, Modification of the Polaron sputter-coater unit for glow-discharge activation of carbon support films, J. Electron Microsc. Tech. 16 (1990) 235–239.
[31] T. Cajka, O. Fiehn, Increasing lipidomic coverage by selecting optimal mobile-phase modifiers in LC-MS of blood plasma, Metabolomics 12 (2016).
[32] H. Tsugawa, T. Cajka, T. Kind, Y. Ma, B. Higgins, K. Ikeda, M. Kanazawa, J. VanderGheynst, O. Fiehn, M. Arita, MS-DIAL: data-independent MS/MS deconvolution for comprehensive metabolome analysis, Nat. Methods 12 (2015) 523–526.
[33] T. Cajka, J.T. Smilowitz, O. Fiehn, Validating quantitative untargeted lipidomics across nine liquid chromatography-high-resolution mass spectrometry platforms, Anal. Chem. 89 (2017) 12360–12368.
[34] C. Dietrich, L.A. Bagatolli, Z.N. Volovyk, N.L. Thompson, M. Levi, K. Jacobson, E. Gratton, Lipid rafts reconstituted in model membranes, Biophys. J. 80 (2001) 1417–1428.
[35] T. Parasassi, G. Destasio, G. Ravagnan, R.M. Rusch, E. Gratton, Quantitation of lipid phases in phospholipid-vesicles by the generalized polarization of Laurdan fluorescence, Biophys. J. 60 (1991) 179–189.
[36] M. Viard, J. Gallay, M. Vincent, M. Paternostre, Origin of laurdan sensitivity to the vesicle-to-micelle transition of phospholipid-octylglucoside system: a time-resolved fluorescence study, Biophys. J. 80 (2001) 347–359.
[37] H.J. Kaiser, D. Lingwood, I. Levental, J.L. Sampaio, L. Kalvodova, L. Rajendran, K. Simons, Order of lipid phases in model and plasma membranes, Proc. Natl. Acad. Sci. U. S. A. 106 (2009) 16645–16650.
[38] M. Shinitzky, Y. Barenholz, Dynamics of the hydrocarbon layer in liposomes of lecithin and sphingomyelin containing dicetylphosphate, J. Biol. Chem. 249 (1974) 2652–2657.
[39] S.C. Lee, T.J. Knowles, V.L.G. Postis, M. Jamshad, R.A. Parslow, Y.P. Lin, A. Goldman, P. Sridhar, M. Overduin, S.P. Muench, T.R. Dafforn, A method for detergent-free isolation of membrane proteins in their local lipid environment, Nat. Protoc. 11 (2016) 1149–1162.
[40] I. Prabudiansyah, I. Kusters, A. Caforio, A.J.M. Driessen, Characterization of the annular lipid shell of the Sec translocon, BBA-Biomembranes 1848 (2015) 2050–2056.
[41] J.M. Dorr, M.C. Koorengevel, M. Schafer, A.V. Prokofyev, S. Scheidelaar, E.A. van der Cruijsen, T.R. Dafforn, M. Baldus, J.A. Killian, Detergent-free isolation, characterization, and functional reconstitution of a tetrameric K + channel: the power of native nanodiscs, Proc. Natl. Acad. Sci. U. S. A. 111 (2014) 18607–18612.
[42] V. Horejsi, K. Drbal, M. Cebecauer, J. Cerny, T. Brdicka, P. Angelisova, H. Stockinger, GPI-microdomains: a role in signalling via immunoreceptors, Immunol. Today 20 (1999) 356–361.
[43] T. Brdicka, J. Cerny, V. Horejsi, T cell receptor signalling results in rapid tyrosine phosphorylation of the linker protein LAT present in detergent-resistant membrane microdomains, Biochem. Biophys. Res. Commun. 248 (1998) 356–360.
[44] D. Filipp, M. Julius, Lipid rafts: resolution of the "fyn problem"? Mol. Immunol. 41 (2004) 645–656.
[45] A.O. Oluwole, B. Danielczak, A. Meister, J.O. Babalola, C. Vargas, S. Keller, Solubilization of membrane proteins into functional lipid-bilayer nanodiscs using a diisobutylene/maleic acid copolymer, Angew. Chem. Int. Ed. 56 (2017) 1919–1924.